ORIGINAL RESEARCH

Investigation of Gray Matter Changes Using Voxel-Based Morphometry in HIV-Negative Patients with General Paresis of the Insane

Hui Chen, Jing-Jing Li, Chun-Shuang Guan, Ming Xue, Yu-Xue Xing, Ru-Ming Xie

Department of Radiology, Beijing Ditan Hospital, Capital Medical University, Beijing, People's Republic of China

Correspondence: Ru-Ming Xie, Department of Radiology, Beijing Ditan Hospital, Capital Medical University, Beijing, 100015, People's Republic of China, Email ch0002018@126.com

Purpose: To investigate whole-brain gray matter volume (GMV) changes in human immunodeficiency (HIV)-negative patients with general paresis of the insane (GPI) using voxel-based morphometry (VBM).

Patients and Methods: A total of 18 HIV-negative individuals with GPI and 24 healthy control volunteers matched for sex, age, and education were enrolled in this study. 3 D T1-weighted imaging (3D T1WI) structural images of GPI patients and healthy controls were preprocessed using VBM. The GMV was then segmented and compared between the two groups. In addition, the correlation between cortical/subcortical GMVs and neuropsychological/laboratory test results was analyzed.

Results: Compared to the normal control group, the GPI group showed a decrease in GMV in multiple regions, including the bilateral frontal cortices (superior frontal gyrus, middle frontal gyrus, orbital gyrus), bilateral temporal/occipital cortices (superior temporal, bilateral inferior temporal, bilateral parahippocampal, bilateral cingulate, left precentral, left fusiform, left posterior superior temporal sulcus, left lateral occipital, right middle temporal, right precuneus, right insular, and right medioventral occipital), and right parietal cortices (right superior parietal, right inferior parietal) ($p < 0.01$, FDR corrected). Additionally, there was an increase in GMV in the bilateral basal ganglia, right hippocampus, and bilateral thalamus ($p < 0.01$, FDR corrected). In the GPI group, GMVs of the right rostral hippocampus ($r = -0.524$, $p = 0.026$), bilateral dorsal caudate nucleus ($r = -0.604$, $p = 0.008$; $r = -0.685$, $p = 0.002$), and the right rostral temporal thalamus ($r = -0.560$, $p = 0.016$) were negatively correlated with MMSE score.

Conclusion: VBM showed that there are structural changes in brain GMV in HIV-negative GPI patients. The use of VBM has the potential to provide a valuable imaging basis for the diagnosis of GPI.

Keywords: neurosyphilis, magnetic resonance imaging, general paresis of the insane, voxel-based morphometry, gray matter

Introduction

Syphilis is prevalent worldwide, with 10.6 million new cases reported annually by the WHO, and the incidence of General paresis of the insane (GPI) has been rising in recent years.[1] The skin lesions of syphilis patients, as well as their secretions and blood contain syphilis spirochetes, and uninfected people can be infected by small breaks in the skin or mucous membranes during sexual contact with a syphilis patient, and very rarely through blood transfusions or other means of transmission. It is called the great imitator because of the numerous clinical symptoms it displays, including cognitive impairment, motor dysfunction, and neuropsychiatric symptoms.[2]

"Neurosyphilis" refers to central nervous system (CNS) infection caused by *Treponema pallidum* subspecies *T. pallidum*,[3,4] and patients may present with CNS manifestations at any time during the course of syphilis. CNS involvement in syphilis patients is classified into four syndromes: syphilitic meningitis, meningovascular syphilis, parenchymatous neurosyphilis, and gummatous neurosyphilis.[5] GPI is a late-onset parenchymal neurosyphilis that can cause progressive dementia.[6] However, it can be cured with appropriate antibiotics. Advanced lesions in GPI can become irreversible due to neuron loss and permanent axon damage. Patient prognosis during treatment can be predicted by

assessing the presence of brain atrophy, particularly in the medial temporal lobe, as detected by magnetic resonance imaging (MRI).[7] But early diagnosis and treatment are crucial. In patients with GPI, neuroimaging abnormalities may provide more reliable information than laboratory results, as false negatives and false positives are inevitable in laboratory assessment of syphilis.[8] Because the CNS manifestations of neurosyphilis are diverse and nonspecific, accurate diagnosis remains problematic.

Voxel-based morphometry (VBM) is based on MRI, which provides detailed anatomical images of the brain. The basic concept of VBM is to analyze differences in the local composition of brain tissues (such as gray matter, white matter, and cerebrospinal fluid) at the voxel level. A voxel is a three-dimensional unit of volume, similar to a pixel in a two-dimensional image, but it represents a volume element in a three-dimensional space. By comparing the distribution and density of voxels representing different tissue types between groups of individuals - such as patients with a neurological disorder and healthy controls, it is possible to identify regions of the brain that may have undergone structural changes due to disease, development, or other factors. The technique has been applied to many different disorders, including neurodegenerative diseases, movement disorders, epilepsy, multiple sclerosis, and schizophrenia.[9–13] It helps to understand the changes occurring in the brain associated with these disorders and elucidates the relationship between these brain changes and the characteristic clinical features.

In a quantitative study of gray matter volume in patients with neurosyphilis, Zi-Ning Lu et al[14] analyzed the gray matter (GM) microstructure of patients with early-stage neurosyphilis using VBM. The results showed regional reductions in GM volume in the left frontal cortex and bilateral temporal/occipital cortex in patients with neurosyphilis, which may be associated with cognitive impairment and intracranial infection, and may be useful for understanding the underlying neural characteristic of neurosyphilis. While many studies have reported clinical and neuroimaging findings in HIV-negative patients with neurosyphilis, little attention has been paid to quantitative brain gray matter volume (GMV) characteristics about GPI. Here, we present our findings in eighteen HIV-negative patients with GPI and discuss the potential value of GM alterations in the diagnosis of GPI. In the present study, we evaluated GM alterations in HIV-negative patients with GPI and controls using VBM analysis.

Materials and Methods

Participants

A total of 18 patients with GPI were enrolled from March 2018 to September 2019. The diagnosis of GPI was based on serological tests and cerebrospinal fluid analysis. HIV antibodies were negative in all patients. *Treponema pallidum* particle asset (TPPA) or rapid plasma reagent (RPR) test results were positive in all patients, and syphilis toluidine red unheated serum test (TRUST) results were also positive. Patients with other potential causes, such as hypertension, diabetes, and related neurological symptoms and signs, were excluded.

Age-, sex-, and education-matched healthy volunteers were included as controls. All control participants had a Mini-Mental State Examination (MMSE) score of 27 or higher. The inclusion criteria for the control participants were as follows: (1) no cognitive impairment or neurological symptoms and no history of systemic, mental, or neurological diseases; (2) no positive signs on physical examination of the nervous system; and (3) no abnormal signs on brain MRI.

The study was approved by the ethics committees of our hospital, and all participants provided written informed consent.

MRI Scan Parameters

Participants underwent MRI scanning using a 3.0 T MRI system (Discovery 750w GE Healthcare) with the following sequences: T1W and T2W axial imaging, T1W sagittal imaging, fast fluid attenuated inversion recovery (FLAIR), and T1-weighted 3D axial IR-prepped FSPGR (BRAVO) sequences. The resulting slices were 1.0 mm thick and were contiguous. The in-plane spatial resolution of the coronal slices was 0.5×0.5×1 mm/pixel. The field of view was 256 mm × 256 mm, and the matrix size was 512×512. The flip angle was 15°, the TR was 7.472 ms, the TE was 2.796 ms, and the TI was 450 ms.

VBM Analyses

MR images were analyzed using FreeSurfer v5.0.9, a set of automated tools. FreeSurfer enables automatic reconstruction of the cortical surface using T1-weighted MR images. The analysis process involves several key steps, including removal of non-brain tissue, automated Talairach transformation, segmentation of subcortical and cortical matter, intensity correction, and delineation of gray/white/pial boundaries. Once cortical models are generated, deformable procedures such as cortical inflation, registration to a spherical atlas, and parcellation of the cerebral cortex into gyral and sulcal units are applied. After initial processing by FreeSurfer, all MRI scans were meticulously examined slice by slice to ensure accurate registration of gray and white matter voxels. Any errors found were corrected, and the scans were reprocessed and subjected to a second visual inspection.

Statistical Analyses

All the statistical analyses were performed using the Statistical Package for the Social Sciences version 25 (SPSS 25) to identify the significant vertex clusters. Differences in GMV were evaluated by two-sample t-tests with age and sex as covariates. The statistical significance of group differences was set at $p < 0.01$ with correction for false discovery rate (FDR). Pearson's correlation analysis was used to examine the relationship between the GMV of each brain atlas and the MMSE score in the GPI group. The significance level was set at $p < 0.05$.

Results

Clinical Data

All patients included in the study were male, ranging in age from 21 to 68 years (mean: 49.2 years). The duration of the disease ranged from 3 months to 7 years. Among the GPI patients, 15 had elevated cerebrospinal fluid white blood cell (CSF-WBC) counts and cerebrospinal fluid total protein (TP) levels. In all patients, memory loss and mood abnormalities were the main manifestations (Figure 1). The control group consisted of 24 men aged 28 to 67 years (mean age: 52.1 years). Table 1 shows the general clinical data and laboratory test results of the 18 GPI patients and 24 normal controls.

GMV Comparison

Compared to the normal control group, the GPI group showed a decrease in GM volume in multiple regions, including the bilateral frontal cortices (superior frontal gyrus, middle frontal gyrus, orbital gyrus), bilateral temporal/occipital cortices (superior temporal, bilateral inferior temporal, bilateral parahippocampal, bilateral cingulate, left precentral, left
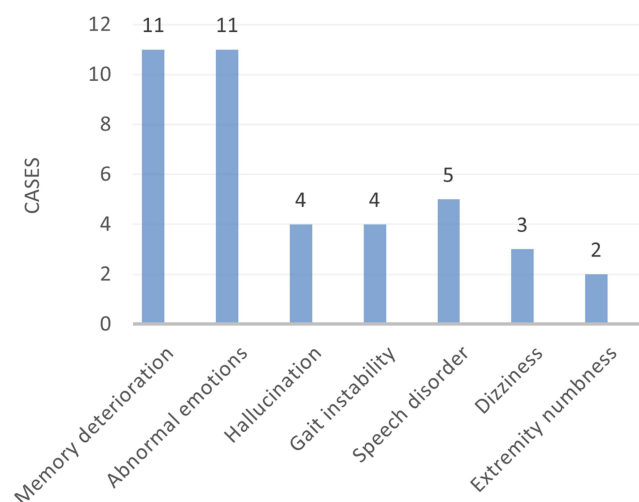

Figure 1 Clinical symptoms and signs of HIV-negative GPI patients (n=18).

Table 1 Demographics, Laboratory Test Results, and Neuropsychological Test Results of the Participants

	GPI (n=18)	HCs (n=24)	t value	P value
Male	18	24	NA	NA
Age (years)	49±12	52±9	0.033	0.974
Education (years)	11±3	11±4	0.012	0.990
MMSE	20.78±7.64	29.58±0.65	−5.64	0.000
Serum RPR titer	50.44±60.23	NA	NA	NA
CSF titer	5.17±7.12	NA	NA	NA
CSF protein concentration (mg/L)	59.22±24.72	NA	NA	NA
CSF WBC count (/μL)	21.17±21.98	NA	NA	NA

Abbreviations: MMSE, Mini-Mental State Examination; RPR, rapid plasma regain; NA, not applicable; CSF, cerebrospinal fluid; WBC, white blood cell.

fusiform, left posterior superior temporal sulcus, left lateral occipital, right middle temporal, right precuneus, right insular, right medioventral occipital), and right parietal cortices (right superior parietal, right inferior parietal) (p<0.01, FDR corrected). In addition, there was an increase in GMV in the bilateral basal ganglia, right hippocampus, and bilateral thalamus (p<0.01, FDR corrected) (Figure 2, Tables 2 and 3).
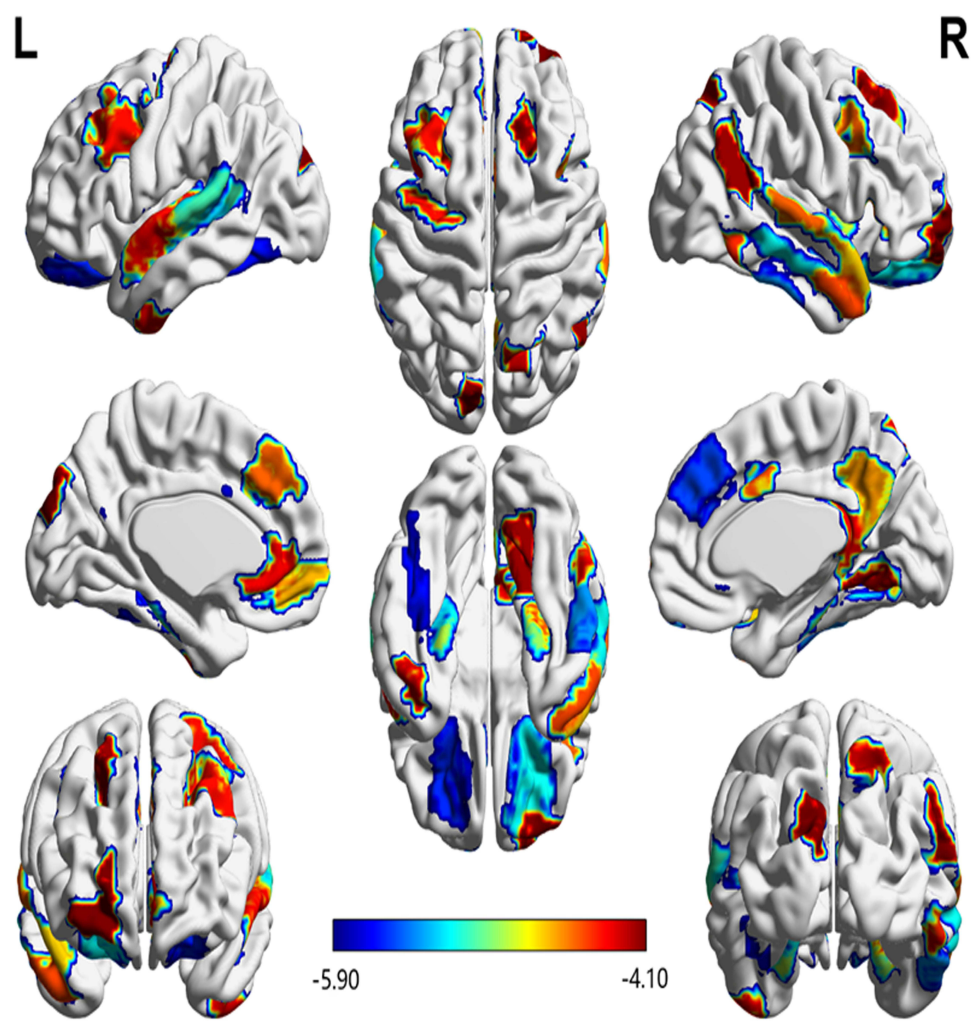

Figure 2 GMV alterations in GPI group compared with normal controls. Red–yellow and blue-light blue color maps indicate GM atrophy and expansion, respectively, in GPI patients compared with normal controls.

Table 2 GMV Differences Between Patients with GPI and Healthy Controls

Hemisphere	Anatomical Site	MNI Coordinates/mm	GPI Group (n=18)	HC Group (n=24)	t values	p values
		X, Y, Z	Mean±Std (mm³)	Mean±Std (mm³)		
Left	Superior Frontal Gyrus	−5, 36, 38	2,253.83±495.90	2,816.25±290.84	−4.49	0.0005
	Middle Frontal Gyrus	−42, 13, 36	2,405.11±561.37	3,152.83 ±519.01	−4.35	0.0007
	Middle Frontal Gyrus	−33, 23, 45	2,424.89±619.78	3,165.50 ±461.52	−4.33	0.0007
	Orbital Gyrus	−7, 54, −7	1,763.28±381.98	2,271.88 ±312.79	−4.63	0.0005
	Orbital Gyrus	−23, 38, −18	2,825.89±525.31	3,614.04 ±363.96	−5.60	0.0001
	Orbital Gyrus	−10, 18, −19	3,224.39±569.69	4,128.63±320.01	−5.89	0.0001
	Precentral Gyrus	−32, −9, 58	1,981.39±481.78	2,605.08 ±425.90	−4.33	0.0007
	Superior Temporal Gyrus	−54, −32, 12	1,403.06±311.50	1,963.13 ±347.07	−5.28	0.0001
	Superior Temporal Gyrus	−50, −11, 1	2,711.72±454.99	3,456.38 ±586.96	−4.36	0.0007
	Superior Temporal Gyrus	−62, −33, 7	1,690.61±466.93	2,442.04 ±458.19	−5.09	0.0002
	Superior Temporal Gyrus	−55, −3, −10	2,247.33±487.24	3,049.46 ±652.28	−4.28	0.0007
	Inferior Temporal Gyrus	−43, −2, −41	1,625.67±484.43	2,176.96 ±334.47	−4.25	0.0007
	Fusiform Gyrus	−42, −51, −17	2,819.39±726.57	4,017.00 ±607.88	−5.67	0.0001
	Parahippocampal Gyrus	−25, −25, −26	413.56±149.75	607.67 ±99.19	−4.92	0.0003
	Parahippocampal Gyrus	−28, −32, −18	457.28±160.81	683.67 ±88.56	−5.25	0.0003
	Posterior Superior Temporal Sulcus	−54, −40, 4	939.94±274.16	1,352.71 ±220.13	−5.28	0.0001
	Posterior Superior Temporal Sulcus	−52, −50, 11	1,072.44±308.85	1,532.88 ±258.66	−5.12	0.0002
	Cingulate Gyrus	−4, 39, −2	1,497.67±508.46	2,161.46 ±466.03	−4.29	0.0007
	Lateral Occipital Cortex	−11, −88, 31	1,650.06±412.20	2,135.13 ±335.17	−4.10	0.0010
	Basal Ganglia	−17, 3, −9	1,743.50±289.99	2,071.67 ±148.25	−4.27	0.0016
	Basal Ganglia	−23, 7, −4	1,804.39±212.43	2,005.83 ±177.11	−3.27	0.0067
	Basal Ganglia	−14, 2, 16	5,177.72±1655.73	3,912.17±624.96	3.35	0.0058
	Basal Ganglia	−28, −5, 2	2,378.56±382.14	2,716.92±195.25	−3.34	0.0077
	Thalamus	−15, −28, 4	1,424.89±164.48	1,673.63±147.8	−5.02	0.0003
Right	Superior Frontal Gyrus	22, 26, 51	1,907.00±319.04	2,310.50 ±293.31	−4.15	0.0009
	Superior Frontal Gyrus	6, 38, 35	2,624.61±555.85	3,515.21 ±461.76	−5.53	0.0001
	Middle Frontal Gyrus	42, 11, 39	1,666.94±498.70	2,259.50 ±334.38	−4.49	0.0005
	Middle Frontal Gyrus	25, 61, −4	3,259.50±782.46	4,116.21 ±534.60	−4.11	0.0010
	Inferior Frontal Gyrus	42, 22, 3	1,747.39±379.74	2,208.33 ±264.14	−4.52	0.0005
	Orbital Gyrus	23, 36, −18	3,845.22±655.99	4,815.13 ±522.96	−5.20	0.0002
	Superior Temporal Gyrus	66, −20, 6	1,687.17±611.83	2,414.04 ±402.35	−4.52	0.0005
	Superior Temporal Gyrus	47, 12, −20	2,238.33±413.44	2,785.25 ±324.60	−4.69	0.0004
	Superior Temporal Gyrus	56, −12, −5	559.83±222.66	814.63 ±131.02	−4.53	0.0005
	Middle Temporal Gyrus	65, −29, −13	1,857.78±723.04	2,860.00 ±383.02	−5.20	0.0003
	Middle Temporal Gyrus	51, 6, −32	2,965.17±894.28	4,020.63 ±450.06	−4.47	0.0009
	Inferior Temporal Gyrus	53, −52, −18	429.72±230.76	744.83 ±232.36	−4.26	0.0007
	Inferior Temporal Gyrus	54, −57, −8	641.17±301.34	1,184.96 ±478.64	−4.40	0.0007
	Inferior Temporal Gyrus	54, −31, −26	1,910.50±508.74	2,694.88 ±411.18	−5.39	0.0001
	Parahippocampal Gyrus	26, −23, −27	421.67±158.48	635.75 ±114.51	−4.96	0.0003
	Parahippocampal Gyrus	30, −30, −18	445.22±136.79	643.79 ±143.93	−4.41	0.0006
	Superior Parietal Lobule	19, −69, 54	1,691.72±346.38	2,106.88 ±275.98	−4.22	0.0008
	Inferior Parietal Lobule	53, −54, 25	3,508.94±1116.24	4,682.96 ±665.51	−4.14	0.0009
	Precuneus	6, −54, 35	2,238.83±807.65	3,169.50 ±465.77	−4.59	0.0005
	Insular Gyrus	38, 5, 5	830.39±207.60	1,131.75 ±185.51	−4.83	0.0003
	Cingulate Gyrus	9, −44, 11	1,144.67±386.77	1,575.29 ±244.80	−4.30	0.0007
	Cingulate Gyrus	4, 6, 38	640.28±293.54	986.75 ±198.11	−4.45	0.0006
	Medioventral Occipital Cortex	18, −60, −7	2,145.28±723.94	3,007.79 ±588.12	−4.15	0.0009
	Hippocampus	22, −12, −20	4,069±604.66	3,560.58±347.18	3.35	0.0058
	Basal Ganglia	15, 8, −9	2,024.67±316.21	2,393.63±163.79	−4.79	0.0003
	Basal Ganglia	22, 8, −1	1,227.11±192.72	1,493.63±106.38	−5.15	0.0003

(Continued)

Table 2 (Continued).

Hemisphere	Anatomical Site	MNI Coordinates/mm	GPI Group (n=18)	HC Group (n=24)	t values	p values
		X, Y, Z	Mean±Std (mm^3)	Mean±Std (mm^3)		
	Basal Ganglia	14, 5, 14	6,515.67±2035.65	4,766.38±1000.14	3.57	0.0042
	Basal Ganglia	29, −3, 1	2,364.17±465.13	2,853.17±266.38	−3.89	0.0034
	Thalamus	3, −13, 5	1,326±316.08	961±134.73	4.47	0.0014
	Thalamus	13, −27, 8	877.39±119.88	1,004.83±110.62	−3.48	0.0049
	Thalamus	10, −14, 14	1,375±171.3	1,157.08±162.25	4.10	0.0014

Abbreviations: MNI, Montreal Neurological Institute; GPI, general paresis of the insane; HC, healthy control.

Table 3 Differences in Deep GMVs (Mean ± SD)

Hemisphere	Anatomical site	MNI Coordinates/mm	GPI (n=18)	HC (n=24)	t	p
		X, Y, Z	Mean±Std (mm^3)	Mean±Std (mm^3)		
Left	Basal Ganglia	−17, 3, −9	1,743.50±289.99	2,071.67±148.25	−4.27	0.0016
	Basal Ganglia	−23, 7, −4	1,804.39±212.43	2,005.83±177.11	−3.27	0.0067
	Basal Ganglia	−14, 2, 16	5,177.72±1,655.73	3,912.17±624.96	3.35	0.0058
	Basal Ganglia	−28, −5, 2	2,378.56±382.14	2,716.92±195.25	−3.34	0.0077
	Thalamus	−15, −28, 4	1,424.89±164.48	1,673.63±147.8	−5.02	0.0003
Right	Hippocampus	22, −12, −20	4,069±604.66	3,560.58±347.18	3.35	0.0058
	Basal Ganglia	15, 8, −9	2,024.67±316.21	2,393.63±163.79	−4.79	0.0003
	Basal Ganglia	22, 8, −1	1,227.11±192.72	1,493.63±106.38	−5.15	0.0003
	Basal Ganglia	14, 5, 14	6,515.67±2,035.65	4,766.38±1,000.14	3.57	0.0042
	Basal Ganglia	29, −3, 1	2,364.17±465.13	2,853.17±266.38	−3.89	0.0034
	Thalamus	3, −13, 5	1,326±316.08	961±134.73	4.47	0.0014
	Thalamus	13, −27, 8	877.39±119.88	1,004.83±110.62	−3.48	0.0049
	Thalamus	10, −14, 14	1,375±171.3	1,157.08±162.25	4.10	0.0014

Correlations Between GM Volumes and MMSE Scores

In the GPI group, the GM volumes of the right rostral hippocampus (r = −0.524, p = 0.026), bilateral dorsal caudate nucleus (r = −0.604, p = 0.008; r = −0.685, p = 0.002), and right rostral temporal thalamus (r = −0.560, p = 0.016) showed significant negative correlations with the MMSE scores (Figure 3A–D). However, there were no significant correlations between GMV and MMSE scores in other brain regions.

Discussion

VBM is a voxel-based method for studying the morphology of brain structures.[15,16] This method reflects the differences in the corresponding anatomical structure by calculating the density change of a certain voxel in unit volume. VBM is a measurement method that can automatically, comprehensively, and objectively analyze changes in the whole brain microstructure.[17] In this study, we evaluated changes in the gray matter of GPI patients using VBM analysis.

Untreated paralytic dementia can occur in all stages of syphilis.[18] In our study, the clinical findings included memory deterioration (11 [61%] of 18), abnormal emotions (11 [61%] of 18), speech disorders (5 [28%] of 18), hallucinations (4 [22%] of 18), gait instability (4 [22%] of 18), dizziness (3 [17%] of 18), and numbness of the extremities (2 [11%] of 18). The study by Yingxin et al showed that high CSF protein levels were an important marker for the diagnosis of neurosyphilis.[19] Similarly, the 18 GPI patients in our study had elevated CSF protein levels and elevated CSF WBC counts.

In this study, compared with healthy controls, HIV-negative GPI patients exhibited reduced gray matter volume in multiple brain regions, particularly in the bilateral frontal, temporal and occipital lobes. Previous research has shown that MRI scans of HIV-negative individuals with neurosyphilis show brain atrophy in the frontal, temporal, and medial
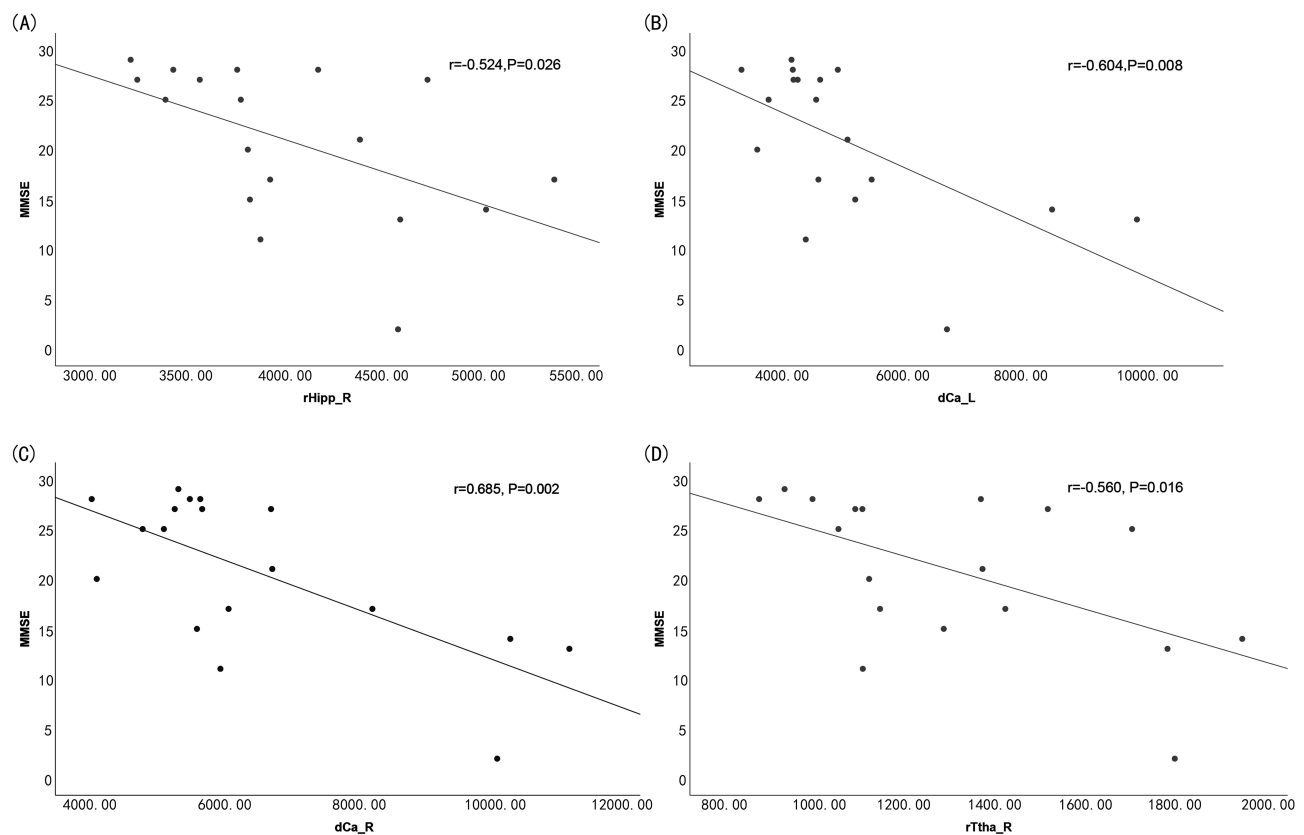
Figure 3 Correlations between neuroimaging data and neuropsychiatric metrics in patients with GPI. (**A**) GMV in the right rostral hippocampus (rHipp_R) was negatively correlated with the MMSE score. (**B**) GMV in the left dorsal caudate nucleus (dCa_L) was negatively correlated with the MMSE score. (**C**) GMV in the right dorsal caudate nucleus (dCa_R) was negatively correlated with the MMSE score. (**D**) GMV in the right rostral temporal thalamus (rTtha_R) was negatively correlated with the MMSE score.

temporal lobes,[7,20] which is consistent with the findings of this study. The potential mechanism involves the direct invasion of *Treponema pallidum* into nerve tissue, leading to widespread brain atrophy, degeneration, neuronal loss, glial cell proliferation, and cortical atrophy. Damage to the frontal lobes may be associated with the development of psychiatric symptoms, dementia, and dysarthria.[18,20] The superior and middle frontal gyri are implicated in motor activity, working memory, and cognitive control.[21,22] Clinical evidence indicates that the superior temporal gyrus plays a crucial role in language production, interpretation, and self-monitoring and is believed to be the neurological foundation for language-related psychotic symptoms in patients.[23] The inferior temporal gyrus is associated with vision, language, and emotion. These findings suggest that the frontal and temporal cortices are essential for memory, cognition, and language and that a decrease in gray matter volume in the frontal and temporal lobes may contribute to the neuropathology of memory loss, mood changes, and speech confusion in patients with GPI. Bilateral frontal or temporal lobe atrophy may reflect cortical destruction and loss of neurons in these areas.[24] Chenhui Mao et al suggest that[25] although temporal lobe involvement is clearly neurosyphilis, later spread to the entire brain is inevitable, and symptoms of frontal lobe involvement may appear earlier. Another study showed that initial infection causes the mesial temporal T2-weighted hyperintensity, with no treatment, may disappear at a later stage when the tissues undergo irreversible atrophy.[26] In addition, Pesaresi I et al found that cortical hypointensity on susceptibility-weighted imaging was mostly distributed in the frontal and temporal lobes, which may be related to iron deposits within activated microglia in GPI patients.[27] Severe medial temporal lobe atrophy is associated with severe cognitive impairment and adverse cognitive outcomes in GPI patients.[28] The exact cause of this atrophy in the medial temporal lobe remains unclear, but it may be due to widespread dysfunction of the cerebral cortex, which connects with other brain regions, such as the frontal, temporal, and parietal lobes. When atrophy affects the medial temporal lobe, including the hippocampus, the prognosis for the patient's social functioning may be unfavorable even with appropriate treatment.[7,29] Neurosyphilis is a great

mimicker and it has been reported that neurosyphilis can mimic early-onset Alzheimer 's disease with bilateral hippocampal atrophy.[30] The parahippocampal gyrus and thalamus are integral components of the limbic system and are crucial for memory and emotion regulation. Additionally, the cingulate cortex, precuneus, and thalamus play roles in attention, motivation, emotion, and memory processing.[31,32] Limbic frontal networks, such as the dorsolateral prefrontal cortex, orbitofrontal cortex, and cingulate cortex, are involved in emotional and affective functions.[31–33] Therefore, the decrease in GMV in the bilateral parahippocampal and cingulate gyri may lead to alterations in memory and mood among patients with GPI.

The hippocampus, a crucial component of the septal area-hippocampus-limbic cholinergic circuit, plays a significant role in human learning and memory. This region receives and processes background information, such as temporal and spatial information, from the hippocampal gyrus.[34,35] Dysfunction of this region may underlie memory loss in patients with GPI.[30,36] The caudate nucleus is essential for controlling gait and walking speed. A larger volume of the caudate nucleus may indicate an increase in neurons or glial cells, potentially leading to impaired motor control and unstable walking in patients with GPI.[37]

A reduction in GMV was observed in some occipital and parietal cortices, including the left lateral occipital cortex, right medioventral occipital cortex, superior parietal lobule, and inferior parietal lobule. Reduced gray matter volume in the parietal and occipital lobes in patients with GPI has rarely been reported in previous studies. This new finding suggests that VBM analysis may be more sensitive than conventional MRI for detecting these changes.

The MMSE is a tool used to assess the severity of cognitive impairment. Negative correlations were found between the gray matter volume indices of the right rostral hippocampus ($r = -0.524$, $p = 0.026$), bilateral dorsal caudate nucleus ($r = -0.604$, $p = 0.008$; $r = -0.685$, $p = 0.002$), and right rostral temporal thalamus ($r = -0.560$, $p = 0.002$; $P = 0.016$) and MMSE scores in the GPI group. This finding suggests that as GMV increases in these areas, the neuropsychological symptoms of GPI patients worsen. The basal ganglia is a complex system of nerve nuclei located deep within the brain and connected to the cerebral cortex, thalamus, and brainstem. This region plays a role in higher cognitive functions such as memory, emotion, motor processes, and reward learning. Our findings of increased GMV in the right rostral hippocampus, bilateral dorsal caudate nucleus and the right rostral temporal thalamus have not been previously reported in the literature. Several factors should be considered to explain the regionally increased GMV found in the present study. First, T. pallidum enters the deep tissues by crossing endothelial cell junctions,[38] which then causes meningeal inflammation, increases the permeability of the blood-brain barrier, and causes widespread cerebral congestion, marked microvascular proliferation, and increased blood flow. Some components of cytotoxic and interstitial edema, inflammation, meningeal vasculitis, or microglial hypertrophy may also be present.[39,40] Then, for brain regions at different stages of pathologic change, there may be brain regions with increased or decreased GMV. Second, alterations in GMV may be associated with changes in dendritic, synaptic and neuronal density, as well as increased afferentation in certain regions.[41] Third, some studies have reported that inflammatory and immune mechanisms may be related to brain structures that directly affect neuronal proliferation, migration, differentiation, and apoptosis. Finally, the relatively small sample size of this study and the fact that the patients were all men may be statistically biased, and larger studies are needed to confirm these findings.[42] Further studies are needed to confirm the potential mechanisms of the exact GMV changes in patients with GPI.

Traditional psychiatric diagnosis has been overly reliant on either self-reported measures or clinical rating scales. Whereas VBM is an objective and scientific measurement technique. It may be possible to somewhat objectively quantify the reduction or increase of the frontal, temporal, and basal ganglia GMV in neuropsychiatric complications of syphilis. The combination of epidemiologic history, clinical presentation, positive serologic test for syphilis spirochetes in serum, routine cerebrospinal fluid examination and clinical rating scales may provide some assistance in the clinical diagnosis of GPI. Additionally, the basic treatment for neuropsychiatric symptoms is penicillin G, VBM may be able to evaluate the early detection of the disease, monitor disease progression, and assess treatment response. If it is to be used more routinely in the diagnosis of neuropsychiatric complications of syphilis, in-depth longitudinal studies involving larger sample sizes should be conducted.

This study has several limitations that should be considered. First, the study included only male syphilis patients. Therefore, it is unclear whether there are any differences in GMV between male and female syphilis patients, as this has

not been addressed in the literature. Future studies should continue to explore whether these findings are applicable to female patients and how they affect the progression and manifestation of GPI. Second, the sample size of this study was relatively small, and more prospective studies with larger sample sizes should be conducted to confirm the results of this study. Finally, the study could not explain the observed increase in subcortical gray matter volume in the GPI group.

Conclusion

HIV-negative individuals with GPI showed different gray matter alterations in the cerebral cortex and subcortical structures. The reduction in gray matter volume in GPI patients predominantly affected the bilateral frontal, temporal, limbic, and basal ganglia regions, which may correlate with symptoms such as memory loss, affective disturbances, and motor dysfunction. In addition, the increased gray matter volume in regions such as the right rostral hippocampus, bilateral dorsal caudate nucleus, and right caudal temporal thalamus in GPI patients may be related to neuropsychological symptoms, although further validation in larger studies is needed. VBM has certain value in evaluating GMV in patients with GPI. However, the underlying mechanisms of the observed changes in GMV need to be further investigated.

Abbreviations

GMV, Gray matter volume; HIV, Human immunodeficiency; GPI, General paresis of the insane; VBM, Voxel-based morphometry; 3D T1WI, 3D T1-weighted imaging; TPPA, Treponema pallidum particle asset; RPR, Rapid plasma reagent; TRUST, Toluidine red unheated serum test; MMSE, Mini-Mental State Examination; FLAIR, Fast fluid attenuated inversion recovery; FDR, false discovery rate; CSF-WBC, cerebrospinal fluid white blood cell; TP, total protein.

Data Sharing Statement

The datasets used during the current study are available from the corresponding author on reasonable request.

Ethics Approval and Consent to Participate

All procedures of this study were performed in accordance with the Declaration of Helsinki and were approved by Ethics Committee of Beijing Ditan Hospital (approval no. 2020-024). All participants gave written informed consent prior to taking part in this study.

Acknowledgments

An unauthorized version of the Chinese MMSE was used by the study team without permission, however this has now been rectified with PAR. The MMSE is a copyrighted instrument and may not be used or reproduced in whole or in part, in any form or language, or by any means without written permission of PAR (www.parinc.com).

Author Contributions

All authors made a significant contribution to the work reported, whether that is in the conception, study design, execution, acquisition of data, analysis and interpretation, or in all these areas; took part in drafting, revising or critically reviewing the article; gave final approval of the version to be published; have agreed on the journal to which the article has been submitted; and agree to be accountable for all aspects of the work.

Disclosure

The authors declare that they have no conflicts of interest in this work.

References

1. Drago F, Merlo G, Ciccarese G. et al. Changes in neurosyphilis presentation: a survey on 286 patients. *J Eur Acad Dermatol Venereol*. 2016;30 (11):1886–1900. doi:10.1111/jdv.13753
2. Gao JH, Ding DY, Qi YY, et al. Neuropsychological Features in Patients with General Paresis of the Insane at an Early Stage. *Med Sci Monit*. 2022;28:e938316. doi:10.12659/MSM.938316

3. Hamill MM, Ghanem KG, Tuddenham S. State-of-The-Art Review: neurosyphilis. *Clin Infect Dis*. 2024;78(5):e57. doi:10.1093/cid/ciad437

4. Wu S, Ye F, Wang Y, et al. Neurosyphilis: insights into its pathogenesis, susceptibility, diagnosis, treatment, and prevention. *Front Neurol*. 2023;14:1340321. doi:10.3389/fneur.2023.1340321

5. Gurses C, Bilgic B, Topcular B, et al. Clinical and magnetic resonance imaging findings of HIV-negative patients with neurosyphilis. *J Neurol*. 2007;254(3):368–374. doi:10.1007/s00415-006-0380-z

6. Gao JH, Li WR, Xu DM, et al. Clinical Manifestations, Fluid Changes and Neuroimaging Alterations in Patients with General Paresis of the Insane. *Neuropsychiatr Dis Treat*. 2021;17:69–78. doi:10.2147/NDT.S279265

7. Kodama K, Okada S, Komatsu N, et al. Relationship between MRI findings and prognosis for patients with general paresis. *J Neuropsychiatry Clin Neurosci*. 2000;12(2):246–250. doi:10.1176/jnp.12.2.246

8. Larsen SA, Steiner BM, Rudolph AH. Laboratory diagnosis and interpretation of tests for syphilis. *Clin Microbiol Rev*. 1995;8(1):1–21. doi:10.1128/CMR.8.1.1

9. Whitwell JL. Voxel-based morphometry: an automated technique for assessing structural changes in the brain. *J Neurosci*. 2009;29(31):9661–9664. doi:10.1523/JNEUROSCI.2160-09.2009

10. Whitwell JL, CR J Jr. Comparisons between Alzheimer disease, frontotemporal lobar degeneration, and normal aging with brain mapping. *Top Magn Reson Imaging*. 2005;16(6):409–425. doi:10.1097/01.rmr.0000245457.98029.e1

11. Genç B, Aksoy A, Aslan K. Cortical and subcortical morphometric changes in patients with frontal focal cortical dysplasia type II. *Neuroradiology*. 2024. doi:10.1007/s00234-024-03471-3

12. Abuaf AF, Bunting SR, Klein S, et al. Analysis of the extent of limbic system changes in multiple sclerosis using FreeSurfer and voxel-based morphometry approaches. *PLoS One*. 2022;17(9):e0274778. doi:10.1371/journal.pone.0274778

13. Goel T, Varaprasad SA, Tanveer M, et al. Investigating White Matter Abnormalities Associated with Schizophrenia Using Deep Learning Model and Voxel-Based Morphometry. *Brain Sci*. 2023;13(2):267. doi:10.3390/brainsci13020267

14. Lu ZN, Yao SJ, Cao Y, et al. Aberrant gray matter structure in neurosyphilis without conventional MRI abnormality: a pilot study with voxel and surface-based morphology. *Acta Radiol*. 2023;64(5):1985–1993. doi:10.1177/02841851221142019

15. Ashburner J, Friston KJ. Why voxel-based morphometry should be used. *Neuroimage*. 2001;14(6):1238–1243. doi:10.1006/nimg.2001.0961

16. Davatzikos C. Voxel-based morphometric analysis using shape transformations. *Int Rev Neurobiol*. 2005;66:125–146.

17. Li J, Wang Y, Xu Z, et al. Whole-brain morphometric studies in alcohol addicts by voxel-based morphometry. *Ann Transl Med*. 2019;7(22):635. doi:10.21037/atm.2019.10.90

18. Russouw HG, Roberts MC, Emsley RA, et al. Psychiatric manifestations and magnetic resonance imaging in HIV-negative neurosyphilis. *Biol Psychiatry*. 1997;41(4):467–473. doi:10.1016/S0006-3223(96)00060-1

19. Yu Y, Wei M, Huang Y, et al. Clinical presentation and imaging of general paresis due to neurosyphilis in patients negative for human immunodeficiency virus. *J Clin Neurosci*. 2010;17(3):308–310. doi:10.1016/j.jocn.2009.07.092

20. Zifko U, Wimberger D, Lindner K, et al. MRI in patients with general paresis. *Neuroradiology*. 1996;38(2):120–123. doi:10.1007/BF00604794

21. Briggs RG, Khan AB, Chakraborty AR, et al. Anatomy and white matter connections of the superior frontal gyrus. *Clin Anat*. 2020;33(6):823–832. doi:10.1002/ca.23523

22. Leung HC, Gore JC, Goldman-Rakic PS. Sustained mnemonic response in the human middle frontal gyrus during on-line storage of spatial memoranda. *J Cogn Neurosci*. 2002;14(4):659–671. doi:10.1162/08989290260045882

23. Yamasaki S, Yamasue H, Abe O, et al. Reduced planum temporale volume and delusional behaviour in patients with schizophrenia. *Eur Arch Psychiatry Clin Neurosci*. 2007;257(6):318–324. doi:10.1007/s00406-007-0723-5

24. Chen YY, Zhang YF, Qiu XH, et al. Clinical and laboratory characteristics in patients suffering from general paresis in the modern era. *J Neurol Sci*. 2015;350(1–2):79–83. doi:10.1016/j.jns.2015.02.021

25. Mao C, Gao J, Jin L, et al. Postmortem Histopathologic Analysis of Neurosyphilis: a Report of 3 Cases With Clinicopathologic Correlations. *J Neuropathol Exp Neurol*. 2018;77(4):296–301. doi:10.1093/jnen/nly004

26. Van Eijsden P, Veldink JH, Linn FH, et al. Progressive dementia and mesiotemporal atrophy on brain MRI: neurosyphilis mimicking pre-senile Alzheimer's disease? *Eur J Neurol*. 2008;15(2):14–15. doi:10.1111/j.1468-1331.2007.02018.x

27. Pesaresi I, Sabato M, Doria R, et al. Susceptibility-weighted imaging in parenchymal neurosyphilis: identification of a new MRI finding. *Sex Transm Infect*. 2015;91(7):489–492. doi:10.1136/sextrans-2014-051961

28. Chen B, Shi H, Hou L, et al. Medial temporal lobe atrophy as a predictor of poor cognitive outcomes in general paresis. *Early Interv Psychiatry*. 2019;13(1):30–38. doi:10.1111/eip.12441

29. Pearson JM, Heilbronner SR, Barack DL, et al. Posterior cingulate cortex: adapting behavior to a changing world. *Trends Cognit Sci*. 2011;15 (4):143–151. doi:10.1016/j.tics.2011.02.002

30. Mehrabian S, Raycheva M, Traykova M, et al. Neurosyphilis with dementia and bilateral hippocampal atrophy on brain magnetic resonance imaging. *BMC Neurol*. 2012;12(1):96. doi:10.1186/1471-2377-12-96

31. Ballmaier M, Toga AW, Blanton RE, et al. Anterior cingulate, gyrus rectus, and orbitofrontal abnormalities in elderly depressed patients: an MRI-based parcellation of the prefrontal cortex. *Am J Psychiatry*. 2004;161(1):99–108. doi:10.1176/appi.ajp.161.1.99

32. Ochsner KN, Gross JJ. The cognitive control of emotion. *Trends Cognit Sci*. 2005;9(5):242–249. doi:10.1016/j.tics.2005.03.010

33. Ochsner KN, Ray RD, Cooper JC, et al. For better or for worse: neural systems supporting the cognitive down- and up-regulation of negative emotion. *Neuroimage*. 2004;23(2):483–499. doi:10.1016/j.neuroimage.2004.06.030

34. Eichenbaum H, Yonelinas AP, Ranganath C. The medial temporal lobe and recognition memory. *Annu Rev Neurosci*. 2007;30(1):123–152. doi:10.1146/annurev.neuro.30.051606.094328

35. Gluth S, Sommer T, Rieskamp J, et al. Effective Connectivity between Hippocampus and Ventromedial Prefrontal Cortex Controls Preferential Choices from Memory. *Neuron*. 2015;86(4):1078–1090. doi:10.1016/j.neuron.2015.04.023

36. Thompson PM, Mega MS, Woods RP, et al. Cortical change in Alzheimer's disease detected with a disease-specific population-based brain atlas. *Cereb Cortex*. 2001;11(1):1–16. doi:10.1093/cercor/11.1.1

37. Moreno-Alcazar A, Ramos-Quiroga JA, Radua J, et al. Brain abnormalities in adults with Attention Deficit Hyperactivity Disorder revealed by voxel-based morphometry. *Psychiatry Res Neuroimaging*. 2016;254:41–47. doi:10.1016/j.pscychresns.2016.06.002

38. Lafond RE, Lukehart SA. Biological basis for syphilis. *Clin Microbiol Rev*. 2006;19(1):29–49. doi:10.1128/CMR.19.1.29-49.2006

39. Kitabayashi Y, Ueda H, Narumoto J, et al. Cerebral blood flow changes in general paresis following penicillin treatment: a longitudinal single photon emission computed tomography study. *Psychiatry Clin Neurosci.* 2002;56(1):65–70. doi:10.1046/j.1440-1819.2002.00930.x

40. Jeong YM, Hwang HY, Kim HS. MRI of neurosyphilis presenting as mesiotemporal abnormalities: a case report. *Korean J Radiol.* 2009;10 (3):310–312. doi:10.3348/kjr.2009.10.3.310

41. Alex F, Murat Y, Brian D, et al. Anatomical abnormalities of the anterior cingulate cortex in schizophrenia: bridging the gap between neuroimaging and neuropathology. *Schizophr Bull.* 2009;35(5):973–993. doi:10.1093/schbul/sbn025

42. Shan XX, Ou YP, Pan P, et al. Increased frontal gray matter volume in individuals with prodromal psychosis. *CNS Neurosci Ther.* 2019;25 (9):987–994. doi:10.1111/cns.13143